EJNMMI Research
a SpringerOpen Journal

ORIGINAL RESEARCH Open Access

Noninvasive k_3 estimation method for slow dissociation PET ligands: application to [^{11}C] Pittsburgh compound B

Koichi Sato[1,2], Kiyoshi Fukushi[1], Hitoshi Shinotoh[1,3], Hitoshi Shimada[1,4], Shigeki Hirano[1,5], Noriko Tanaka[6], Tetsuya Suhara[1], Toshiaki Irie[1] and Hiroshi Ito[1*]

Abstract

Background: Recently, we reported an information density theory and an analysis of three-parameter plus shorter scan than conventional method (3P+) for the amyloid-binding ligand [^{11}C]Pittsburgh compound B (PIB) as an example of a non-highly reversible positron emission tomography (PET) ligand. This article describes an extension of 3P + analysis to noninvasive '3P++' analysis (3P + plus use of a reference tissue for input function).

Methods: In 3P++ analysis for [^{11}C]PIB, the cerebellum was used as a reference tissue (negligible specific binding). Fifteen healthy subjects (NC) and fifteen Alzheimer's disease (AD) patients participated. The k_3 (index of receptor density) values were estimated with 40-min PET data and three-parameter reference tissue model and were compared with that in 40-min 3P + analysis as well as standard 90-min four-parameter (4P) analysis with arterial input function. Simulation studies were performed to explain k_3 biases observed in 3P++ analysis.

Results: Good model fits of 40-min PET data were observed in both reference and target regions-of-interest (ROIs). High linear intra-subject (inter-15 ROI) correlations of k_3 between 3P++ (*Y*-axis) and 3P + (*X*-axis) analyses were shown in one NC ($r^2 = 0.972$ and slope = 0.845) and in one AD ($r^2 = 0.982$, slope = 0.655), whereas inter-subject k_3 correlations in a target region (left lateral temporal cortex) from 30 subjects (15 NC + 15 AD) were somewhat lower ($r^2 = 0.739$ and slope = 0.461). Similar results were shown between 3P++ and 4P analyses: $r^2 = 0.953$ for intra-subject k_3 in NC, $r^2 = 0.907$ for that in AD and $r^2 = 0.711$ for inter-30 subject k_3. Simulation studies showed that such lower inter-subject k_3 correlations and significant negative k_3 biases were not due to unstableness of 3P++ analysis but rather to inter-subject variation of both k_2 (index of brain-to-blood transport) and k_3 (not completely negligible) in the reference region.

Conclusions: In [^{11}C]PIB, the applicability of 3P++ analysis may be restricted to intra-subject comparison such as follow-up studies. The 3P++ method itself is thought to be robust and may be more applicable to other non-highly reversible PET ligands with ideal reference tissue.

Keywords: [^{11}C]Pittsburgh compound B; Alzheimer's disease; Kinetic modeling; PET quantification; Reference tissue; Slow dissociation ligand

* Correspondence: hito@nirs.go.jp
[1]Molecular Imaging Center, National Institute of Radiological Sciences, 4-9-1 Anagawa, Inage-ku, Chiba 260-8555, Japan
Full list of author information is available at the end of the article

Background

Various reversible-type radioligands have been developed for *in vivo* neuroreceptor study with positron emission tomography (PET). Both arterial blood sampling and long dynamic PET scan, up to 120 min, are required for standard nonlinear least-squares (NLS) analysis to estimate K_1 to k_4 in the two-tissue compartment four-parameter model (4P model): K_1 represents the blood-to-brain transport constant, k_2 represents the brain-to-blood transport constant, k_3 represents the first-order association rate constant for specific binding, and k_4 represents the dissociation rate constant for specific binding. The k_3 represents $B_{max} \cdot k_{on}$, where B_{max} is maximum receptor density and k_{on} is the *in vivo* association rate constant. Since k_3 represents available receptors for the PET ligand, it is the target parameter of major interest in most PET studies. However, quantification of k_3 in the 4P model is often difficult because of uncertainty of the k_4 estimate and high correlation between the k_3 and k_4 estimates. As surrogate parameters for B_{max}, binding potential and distribution volume have been widely used [1-4]. Several reference tissue methods have also been developed [5-10].

Irreversible (enzyme-substrate type) radiotracers [^{11}C] methylpiperidin-4-yl acetate and propionate have been developed for the measurement of cerebral acetylcholine esterase activity using PET [11,12]. In this case the two-tissue compartment three-parameter (K_1 to k_3) model (3P model) was used to estimate k_3, which is an index of acetylcholine esterase activity. In the 3P model, the precision of k_3 estimate is usually higher than in the 4P model, in spite of shorter PET scan time (40 to 60 min), since there is no need of k_4 estimation in the 3P model.

We have previously defined two mathematical functions, the information density function and information function, which are useful for model selection and optimization of scan time in PET [13]. Based on simulations using both functions, we proposed a new method (3P + method) for quantification of k_3 for moderately reversible ligands. '3P+' means three-parameter model plus short PET scan. In this method, the 3P model ($k_4 = 0$ model) was applied to the early-phase PET data (up to 30 to 40 min) from reversible ligands with moderate k_4 (moderately reversible ligands). Although the 3P + method was not always developed for a specific ligand, the amyloid-binding radiotracer [^{11}C]Pittsburgh compound B (PIB) was used as an example for the moderately reversible ligands (k_4 = 0.018/min). The 3P + method afforded a more stable k_3 estimate than the standard 90-min 4P analysis. However, there is still the drawback of the necessity for arterial blood sampling and radiometabolite analysis, which may restrict the widespread use of this method in daily clinical practice.

In this article, we propose a noninvasive 3P++ analysis using [^{11}C]PIB. 3P++ means 3P + analysis plus use of a reference tissue for input function. To validate the proposed method, the linear correlations of k_3 estimates were evaluated between 40-min 3P++ and 3P + analyses, as well as between 3P++ and 90-min 4P analyses in clinical PET studies. In addition, simulation studies were performed to explain k_3 biases observed in the 3P++ analysis.

Methods

Theory

Assumptions in 3P++ analysis

The following are assumptions used in 3P++ analysis:

- Assumption 1 (on the nature of radioligand used): We apply 3P++ analysis only to moderately reversible or nearly irreversible radioligands ($k_4 \le 0.03$/min), but exclude highly reversible ligands. [^{11}C]PIB is an example of moderately reversible ligands ($k_4 = 0.018$/min).
- Assumption 2 (on the duration time of PET scan): We use early-phase PET data in the curve fitting. In [^{11}C]PIB, dynamic PET data during 0 to 40 min was described well with the 3P model, since the effect of the k_4 process on PET data was negligible within these early-phase kinetics [13].
- Assumption 3 (on the specific binding in the reference tissue, k_{3r}): Specific binding of radioligand is negligible in the reference tissue ($k_{3r} = 0$). In [^{11}C]PIB, the gray matter of the cerebellum is usually used as a reference tissue for input function [14]. We apply the one-tissue compartment two-parameter (K_1, k_2) model (2P model) to the reference tissue.

Working equation for 3P++ analysis

The working equation for the 3P++ analysis has been reported [15]:

$$\begin{aligned} C_t(t) &= R_1\left[\delta(t) + \frac{k_{2r}k_3}{k_2+k_3} + \left(k_{2r} - k_2 - \frac{k_{2r}k_3}{k_2+k_3}\right)e^{-(k_2+k_3)t}\right] \otimes C_r(t) \\ &= R_1 C_r(t) + \frac{R_1 k_{2r} k_3}{k_2+k_3}\int_0^t C_r(\tau)d\tau - \frac{R_1 k_2 (k_2+k_3-k_{2r})}{k_2+k_3} \\ &\quad \times \int_0^t e^{-(k_2+k_3)(t-\tau)} C_r(\tau)d\tau, \end{aligned} \tag{1}$$

where $C_t(t)$ is the radioactivity concentration in the target tissue and $C_r(t)$ is that in the reference tissue; k_{2r} is the k_2 in the reference tissue and $\otimes$ is the convolution integral. The rate of tracer penetration into the target tissue is obtained as the relative value R_1, which is the ratio of target K_1 to reference K_1.

Clinical PET study

Human subjects

Two groups of subjects, a normal control (NC) group and an Alzheimer's disease (AD) group, participated in

the current study with written informed consent. The NC group consisted of 15 healthy subjects (age ranging from 48 to 90 years, 66.7 ± 11.5 years (mean ± SD); eight males and seven females) without a history of central nervous system diseases or psychiatric disorders, and the AD group consisted of 15 patients (ages 55 to 85, 68.9 ± 9.6 years; four males and 11 females) diagnosed as probable AD according to the criteria of the National Institute of Neurological and Communication Disorders, Alzheimer's Disease and Related Disorders Association [16]. The study was approved by the Institutional Review Board of the National Institute of Radiological Sciences.

Radiochemical synthesis

[^{11}C]PIB was synthesized by the reaction of 2-(4′-aminophenyl)-6-hydroxy-benzothiazole and [^{11}C]methyl triflate [17]. The product had radiochemical purity greater than 95.4%. Specific activity was in the range of 56.3 to 285.3 GBq/μmol.

PET scan protocol

PET images were acquired with a Siemens ECAT EXACT HR + scanner (CTI PET systems, Inc., Knoxville, TN, USA) with an axial field of view of 155 mm, providing 63 contiguous 2.46-mm slices with 5.6-mm transaxial and 5.4-mm axial resolution. After a 10-min transmission scan for tissue attenuation correction, infusion of [^{11}C]PIB (about 370 MBq in 5 mL for 1 min) began. A PET scan in 3D mode was started after the arrival of tracer to the brain (approximately 30 s after the beginning of tracer infusion). The dynamic scans consisted of 19 frames (3 × 20 s, 3 × 40 s, 1 × 1 min, 2 × 3 min, 5 × 6 min, and 5 × 10 min) with the total scan duration of 90 min. All data processing and image reconstruction were performed using standard Siemens software, which included scatter correction, randoms, and dead time correction.

Region-of-interest delineation

Region-of-interest (ROI) analysis was performed using the PMOD software package (PMOD version 3.2; Technologies Ltd., Adliswil, Switzerland). The [^{11}C]PIB PET images were co-registered to T_1 weighted images in each subject. The following 15 ROIs were drawn manually on T_1 weighted images: frontal, mesial temporal, lateral temporal, parietal, occipital, anterior cingulate, and posterior cingulate cortices in both hemispheres as well as the reference tissue (gray matter of cerebellum). ROIs were transferred to co-registered [^{11}C]PIB PET images, and time-activity curves (TACs) were obtained in those brain regions.

Input function measurement

During PET scan, arterial blood was collected from radial artery, starting 6 s (transit delay at the blood sampling site) after the beginning of PET scan to 85 min post injection (10 × 10 s, 1 × 30 s, 9 × 2 min, 6 × 10 min, and 1 × 5 min; 27 samples). Radioactive metabolites were analyzed by a radio-thin layer chromatography (TLC) method [12], with a TLC-developing solvent (ethyl acetate/*n*-hexane = 2:1 vols). The metabolite-corrected radioactivity as well as total radioactivity in blood plasma was fitted to a mono-exponential saturation function during infusion (0 to 1 min) and the sum of three-exponential functions after the end of infusion (1 to 85 min) [12].

4P and 3P + analyses (arterial-plasma input)

Brain regional TACs were analyzed by the weighted NLS method under positive constraint of all k_i with metabolite-corrected input function to afford K_1 to k_4 estimates in 4P analysis (scan time of 90 min) and K_1 to k_3 estimates in 3P + analysis (40 min). Correction was made for blood-pool (5%) radioactivity in brain tissue [14]. Custom software operating in IDL software (version 6.0; Jicoux Datasystems, Inc., Tokyo, Japan) environment was used for the compartment model analysis.

3P++ analysis (reference tissue input)

For successful convergence in NLS optimization using Equation 1, we fixed k_{2r} to 0.178/min (mean cerebellar k_2 value by 40-min 3P + analysis; $N = 30$; SD = 0.034). Based on Equation 1 and cerebellar TAC with a fixed k_{2r} value, the time-integral of $C_r(t)$ (the second term on the right side of Equation 1) and the convolution integral (the third term) were calculated numerically without data interpolation for each scan mid-times during 0 to 40 min, and the three parameters R_1, k_2, and k_3 were estimated.

Simulation study

Generation of error-added TACs for Monte Carlo simulation

The error-free, baseline TACs (19 frames/90 min) simulating the target ROI of the NC and AD subjects were generated by using the 4P model with parameter set ($K_1 = 0.180$ mL/g/min, $k_2 = 0.180$/min, $k_3 = 0.018$ and 0.036/min for the NC and AD subjects, respectively, and $k_4 = 0.018$/min; typical values for [^{11}C]PIB) and averaged ($N = 20$) input function of [^{11}C]PIB. The reference ROI was the same between NC and AD subjects and was generated by using the 2P model with parameter set ($K_1 = 0.180$ mL/g/min, $k_2 = 0.180$/min) and the same input function as above. The error-added TACs for simulation were generated according to the following formula [18]:

$$\text{Error-added } C_i = C_i + \text{Rand} \times \sigma(C_i),$$
$$\sigma(C_i) = \varepsilon\sqrt{\frac{C_i}{\Delta t_i \times \exp(-\lambda t_i)}}, \quad (2)$$

where C_i is noise-free simulated radioactivity concentration at frame number i, Rand is a random number from a Gaussian distribution with a mean 0 and variance 1, ε is a

scaling factor that determines the noise level, Δt_i is scan duration of frame number i, t_i is mid-scan time of frame number i, and λ is ^{11}C decay constant. In all Monte Carlo simulations, a data set of 100 noise-added TACs was analyzed with weighted NLS, using a relative weight w_i:

$$w_i = \text{constant} \times \frac{\Delta t_i \times \exp(-\lambda t_i)}{C_i}. \quad (3)$$

Effects of PET noise on 4P, 3P+, and 3P++ analyses

Five levels of PET noise (0.025, 0.05, 0.1, 0.2, and 0.3; ε in Equation 2, relative values empirically determined) were added to the baseline TACs of the target ROI of the NC subjects. From 100 error-added TACs for each PET noise level, 100 k_3 values were estimated using 90-min 4P, 40-min 3P+, and 3P++ analyses. Coefficient-of-variation (CV) of k_3 was calculated as CV (%) = (SD/mean) × 100. In the following simulations, the PET noise was fixed at 0.1.

Effects of K_1 change in target ROI on 4P, 3P+, and 3P++ analyses

Simulated target TACs were generated by 4P model with five different K_1 values (0.12, 0.15, 0.18, 0.21, and 0.24 mL/g/min) and fixed k_3 (0.018/min) and k_4 (0.018/min). The value of K_1/k_2 was fixed at 1. The range of K_1 was determined with clinically measured K_1 for [^{11}C]PIB (0.177 ± 0.31 in NC group and 0.168 ± 0.30 in AD group; 90-min 4P analysis). Reference TAC was the same as baseline reference TAC. The k_3 bias in 90-min 4P, 40-min 3P+, and 3P++ analyses relative to the true k_3 (0.018/min) was calculated as bias (%) = (estimated k_3/true k_3 – 1) × 100.

Effects of k_2 or k_3 change in reference ROI on 3P++ analysis

In 3P++ analysis, k_{3r} was assumed to be 0 and k_{2r} was fixed as an empirical constant. The effects of k_{2r} or k_{3r} change were investigated as follows. The error-added target TACs were generated by 4P model with two different k_3 values (0.018/min for NC and 0.036/min for AD); other parameters were the same as the baseline target TAC. The error-added reference TACs were generated by 2P model with five different k_2 (0.12, 0.15, 0.18, 0.21, and 0.24/min) and fixed K_1 values (0.18 mL/g/min). Another set of simulated reference TACs was generated by 3P model (not 2P model) with five different k_3 (0, 0.002, 0.004, 0.006, and 0.008/min) and fixed K_1 (0.18 mL/g/min) and k_2 (0.18/min). The k_3 bias in 3P++ analysis was expressed relative to 3P + analysis as bias (%) = (3P++ k_3/3P + k_3 – 1) × 100.

Although k_{3r} was assumed to be 0 in Equation 1, each subject may have different k_{3r} values that deviated from 0. In simulations to investigate the effect of the individual k_{3r} variation on 3P++ analysis, we defined the k_3 value empirically corrected for nonzero k_{3r} as follows: $k_3' = k_3 + k_{3r}$, where k_3 is the k_3 estimate of target ROI by 3P++ analysis and k_{3r} is the k_3 estimate of reference ROI by 3P + analysis (true reference k_3). Bias in 3P++ k_3' relative to 3P + k_3 was compared with the bias in 3P++ k_3 to 3P + k_3.

Results

Goodness of model fits in 3P++ analysis

Figure 1A shows an example of the curve fitting of [^{11}C]PIB cerebellar TAC data to the 2P model, where a good fit is seen during 0 to 40 min after tracer injection. Figure 1B shows the fits of cerebral cortical TAC data (0 to 40 min) to the 3P + and 3P++ models. The goodness-of-fit by 3P++ model (reference tissue input) is almost indistinguishable from that by 3P + model (arterial-plasma input). Kinetic parameters (K_1 = 0.161 mL/g/min, k_2 = 0.167/min and

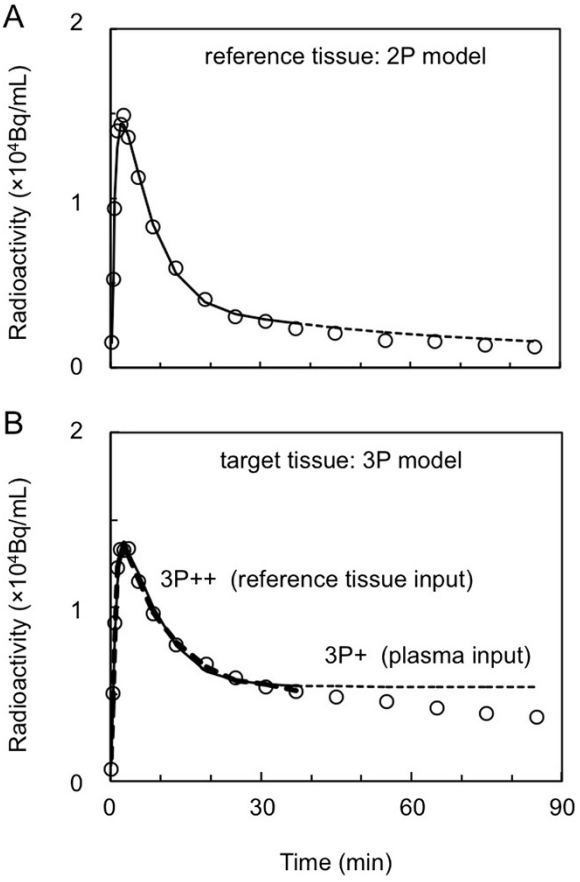

Figure 1 Reference and target tissue TACs in [^{11}C]PIB PET. (A) Cerebellar (reference tissue) data (open circle) up to 90 min in one AD subject and the fit of 40-min data to the 2P model (solid line). **(B)** Cerebral cortical (target tissue) data (open circle) in the same subject and the fits of 40-min data to the 3P model with arterial-plasma input (3P + analysis; solid line) or reference tissue input (3P++ analysis; dashed line). The dotted lines in **(A)** and **(B)** indicate the extension of the solid line from 40 to 90 min.

k_3 = 0.015/min) were estimated in 3P + analysis and R_1 = 0.897, k_2 = 0.158/min and k_3 = 0.011/min in 3P++ analysis.

Intra-subject k_3 correlation

Figure 2A is an example of the intra-subject k_3 correlation between 40-min 3P + (*X*-axis) and 3P++ (*Y*-axis) analyses, where the k_3 values of 15 ROIs, including the cerebellum (reference tissue in 3P++ analysis) from one particular NC subject or one particular AD subject, are shown. The regression lines and the coefficients of determination are $Y = 0.845X - 0.006$ ($r^2 = 0.972$) for the NC subject and $Y = 0.655X - 0.004$ ($r^2 = 0.982$) for the AD subject. Cerebellar k_3 values for both subjects are naturally calculated to be 0 in the 3P++ analysis. The slopes of the regression lines indicate the presence of negative bias in the 3P++ against the 3P + analysis.

Figure 2B shows the k_3 correlation between 90-min 4P (*X*-axis) and 40-min 3P++ (*Y*-axis) analyses in the same subjects. The regression lines are $Y = 0.590X - 0.005$ (r^2 = 0.953) for the NC subject and $Y = 0.338X + 0.000$ (r^2 = 0.907) for the AD subject. When the cerebellar data ($X = 0.008$, $Y = 0.000$) was removed from calculation for the AD subject, the regression line became $Y = 0.295X - 0.002$ with slightly larger r^2 (0.935; not shown in the figure). The slopes of the regression lines show that k_3 bias in 3P++ against 4P analysis is larger than that against 3P + analysis.

Inter-subject k_3 correlation

Figure 3A shows an example of the inter-subject k_3 correlation, where k_3 values for the left lateral temporal cortex from 30 subjects (15 NC + 15 AD) are compared between 40-min 3P + (*X*-axis) and 3P++ (*Y*-axis) analyses. The regression lines are $Y = 0.461X - 0.001$ (r^2 = 0.739) for all 30 subjects, $Y = 0.178X + 0.000$ ($r^2 = 0.151$) for the NC group alone, and $Y = 0.286X + 0.003$ (r^2 = 0.411) for the AD group alone; the latter two lines are not shown in the figure. The slopes of the regression lines also indicate the presence of negative biases in 3P++ against 3P + analysis.

Figure 3B shows the inter-subject correlation of left lateral temporal k_3 between 90-min 4P (*X*-axis) and 40-min 3P++ (*Y*-axis) analyses, where the regression line is $Y = 0.225X + 0.000$ ($r^2 = 0.711$) for all subjects. The lines of $Y = 0.090X + 0.001$ ($r^2 = 0.122$) for the NC group alone and $Y = 0.135X + 0.005$ ($r^2 = 0.513$) for the AD group alone were also calculated. The slopes of the regression lines show larger negative k_3 biases in 3P++ against 4P analysis than that shown in Figure 3A. The results in other cerebral regions were essentially the same as those in the left lateral temporal cortex.

Simulation on the effects of PET noise on k_3 CV

Figure 4 compares the noise sensitivity of k_3 estimates among the 90-min 4P, 40-min 3P+, and 3P++ analyses. In all three analyses, the k_3 CVs increased as the PET error became larger. The k_3 CV in 3P++ analysis was comparable to that in 3P + analysis and lower than that in 4P analysis; for example, k_3 CVs at 0.1 of noise level were 6.6% in 3P++, 7.0% in 3P+, and 11.4% in 4P analyses.

Simulation on the effects of target K_1 change on k_3 bias

Figure 5 shows the effects of K_1 change in the target ROI on the k_3 biases in the 90-min 4P, 40-min 3P+, and 3P++ analyses. The 4P analysis remained almost bias-free (+0.6%) within K_1 from 0.12 to 0.24 mL/g/min. 3P + and 3P++ analyses showed larger negative biases (−33% to −34% bias in 3P + and −33% to −35% bias in 3P++) compared with 4P analysis. Although 3P++ analysis showed slightly larger k_3 bias than 3P + analysis

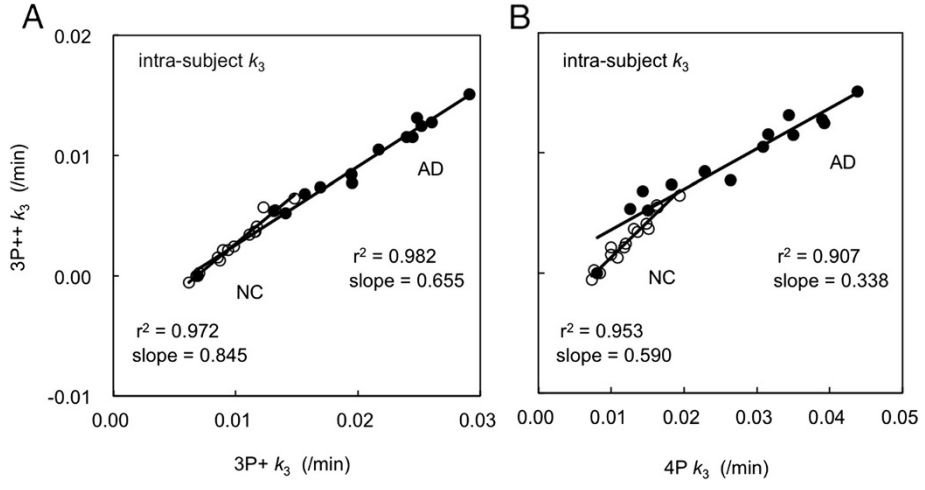

Figure 2 Intra-subject correlation of k_3 for 15 ROIs in [^{11}C]PIB PET. The results in 40-min 3P++ (*Y*-axis) vs. 3P + (*X*-axis) analyses **(A)** and 40-min 3P++ vs. 90-min 4P analyses **(B)** with one NC subject (open circle) and one AD subject (closed circle) are shown.

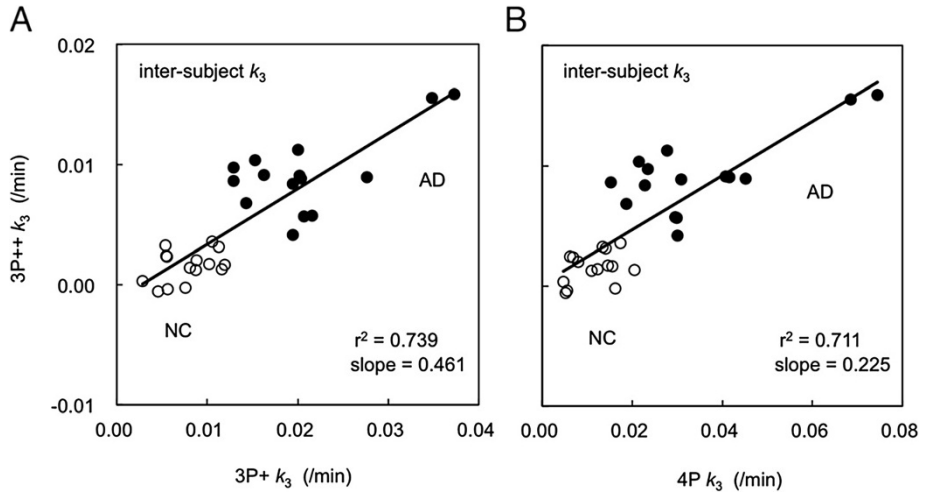

Figure 3 Inter-subject correlations of left lateral temporal k_3 in [^{11}C]PIB PET. The results in 40-min 3P++ (*Y*-axis) vs. 3P + (*X*-axis) analyses **(A)** and 40-min 3P++ vs. 90-min 4P analyses **(B)** with 30 subjects (15 NC, open circle; 15 AD, closed circle) are shown.

when K_1 was low (0.12 mL/g/min), k_3 bias in 3P++ analysis was almost the same as 3P + analysis.

Simulation on the effects of k_{2r} change on 3P++ analysis

In 3P++ analysis (Equation 1), k_{2r} was fixed at 0.178/min, though k_{2r} was not always the same among subjects (CV = 19%). Figure 6 shows the effects of individual k_{2r} change in 40-min 3P++ analysis. When k_{2r} was equal to the fixed value (0.18/min), 3P++ analysis was bias-free, relative to 3P + analysis. However, when k_{2r} was different from the fixed value, 3P++ analysis showed a negative k_3 bias relative to 3P + k_3. The k_{2r} effects were similar between NC ROI (k_3 = 0.018/min) and AD ROI (k_3 = 0.036/min); for example, the biases were −14.1% for NC and −12.1% for AD at k_{2r} = 0.12/min and −14.1% for NC and −11.3% for AD at k_{2r} = 0.24/min.

Simulation on the effects of k_{3r} change on 3P++ analysis

In 3P++ analysis we assume that k_{3r} = 0, that is, specific binding is negligible in the reference tissue. However, in all subjects examined, this assumption did not hold: the k_{3r} values in 40-min 3P + analysis were 0.008 ± 0.004/min in the AD group, 0.007 ± 0.002/min in the NC group, and 0.007 ± 0.003/min in the AD + NC group.

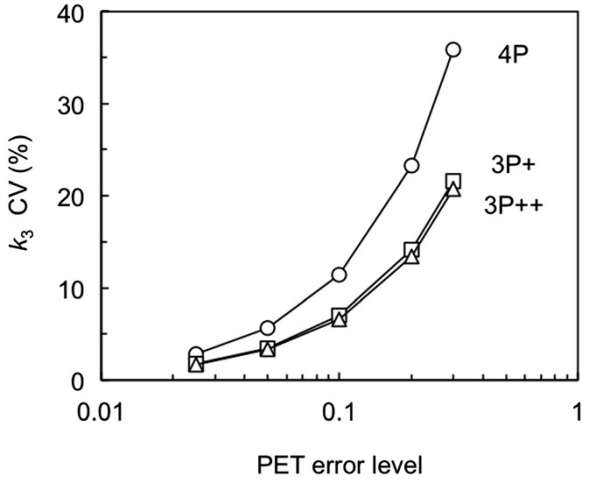

Figure 4 Effects of PET noise on CV of k_3. The results in 40-min 3P++ (open triangle), 40-min 3P + (open square), and 90-min 4P (open circle) analyses are shown. Five different PET noises (0.025 to 0.3) were added to the [^{11}C]PIB baseline TACs of the target ROI of the NC subjects. CV of k_3 was calculated from 100 k_3 estimates as CV (%) = (SD/mean) × 100.

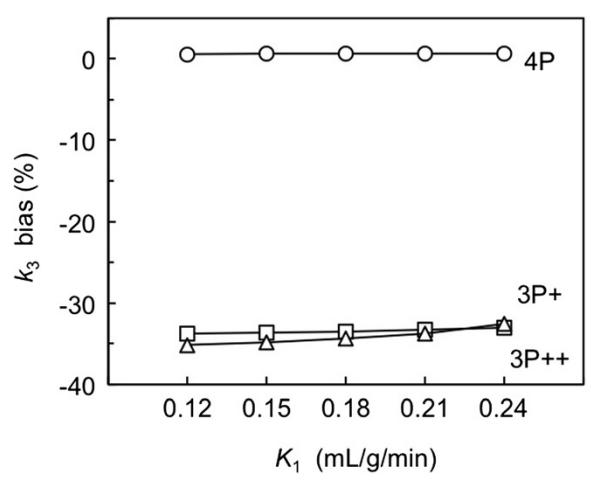

Figure 5 Effects of K_1 change in the target region on k_3 bias. The results in 40-min 3P++ (open triangle), 40-min 3P + (open square) and 90-min 4P (open circle) analyses are shown. Simulated target TACs were generated by 4P model with five different K_1 values (0.12 to 0.24 mL/g/min). The k_3 bias was calculated as bias (%) = (estimated k_3/true k_3 − 1) × 100.

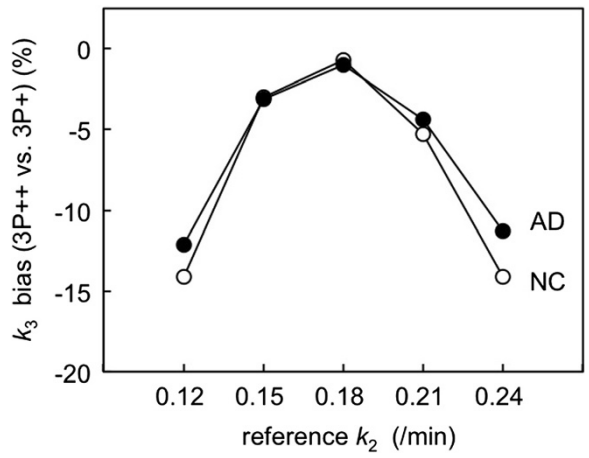

Figure 6 Effects of k_2 change in the reference region on k_3 bias in 40-min 3P++ analysis. Simulated target TACs were generated by 4P model with two different k_3 values (0.018/min for NC, open circle; 0.036/min for AD, closed circle). Simulated reference TACs were generated by 2P model with five different k_2 values (0.12 to 0.24/min). The k_3 bias in 3P++ analysis was expressed relative to 3P + analysis as bias (%) = (3P++ k_3/3P + k_3 − 1) × 100.

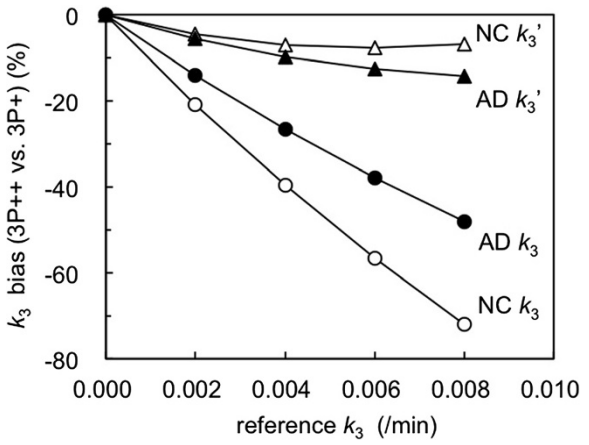

Figure 7 Effects of k_3 change in the reference region on k_3 bias in 40-min 3P++ analysis. Simulated target TACs were generated by 4P model with two different k_3 values (0.018/min for NC, open circle; 0.036/min for AD, closed circle). Simulated reference TACs were generated by 3P model with five different k_3 values (0 to 0.008/min). The k_3 bias in 3P++ analysis was expressed relative to 3P + analysis as bias (%) = (3P++ k_3/3P + k_3 − 1) × 100. Effects on bias in 3P++ k_3′ relative to 3P + k_3 are also shown (NC, open triangle; AD, closed triangle), where 3P++ k_3′ was calculated as (3P++ k_3′) = (3P++ k_3) + reference k_3.

Figure 7 shows the effects of individual k_{3r} change (0 to 0.008/min) on 40-min 3P++ analysis. When k_{3r} was 0, 3P++ analysis was bias-free, relative to 3P + analysis. The k_3 biases (negative biases) increased as k_{3r} increased: −38% for NC and −27% for AD at k_{3r} = 0.004/min and −70% for NC and −48% for AD at k_{3r} = 0.008/min. The NC ROI (k_3 = 0.018/min) showed larger biases than the AD ROI (k_3 = 0.036/min). Figure 7 also shows the results of the simulation study on the relationship between 3P++ k_3′ and 3P + k_3, where 3P++ k_3 was empirically corrected with individual k_{3r}. In this case, negative bias in 3P++ k_3′ was significantly decreased compared to that in 3P++ k_3; for example, bias was decreased from −70% to −7% for NC, and from −48% to −15% for AD at k_{3r} = 0.008/min.

Figure 8 shows the correlation between 3P++ k_3′ and 3P + k_3 using the same data as in Figure 3A, where 3P++ k_3 in Figure 3A was replaced by 3P++ k_3′. The regression line was $Y = 0.678X + 0.003$ ($r^2 = 0.975$) for all subjects, where X = 3P + k_3 and Y = 3P++ k_3′. The lines of $Y = 0.798X + 0.002$ ($r^2 = 0.897$) for the NC group alone and $Y = 0.620X + 0.004$ ($r^2 = 0.960$) for the AD group alone were also calculated. The determination coefficient was increased by this correction from 0.739 to 0.975. The slope of the regression line was also increased from 0.461 (Figure 3A) to 0.678 (Figure 8), which showed the reduction of negative bias in 3P++ analysis.

Discussion

Theoretical basis and merits of 3P++ analysis

The previous 3P + analysis allowed for estimating k_3 of moderately reversible ligands, where the 3P model was applied to early-phase (up to 30 to 40 min) PET data with arterial input function [13]. It was reported that when the 3P model was applied to 60-min PET scan data from [^{11}C]PIB (k_4 = 0.018/min) as a moderately reversible ligand, only a poor model fit was obtained [19]. Previous simulation studies on [^{11}C]PIB using information

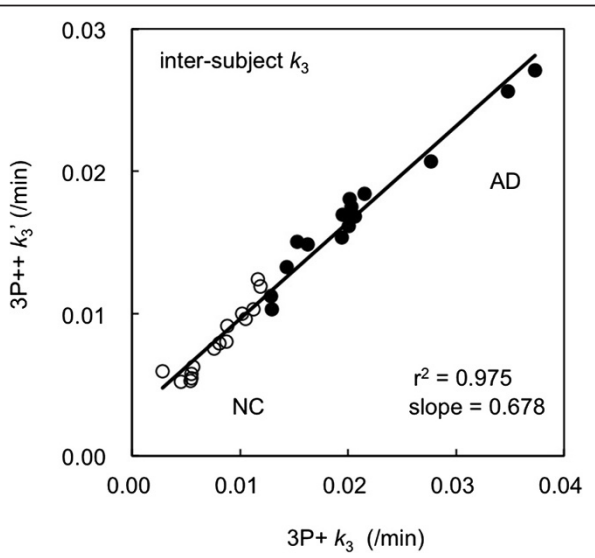

Figure 8 Inter-subject correlation of left lateral temporal k_3 in [^{11}C]PIB PET. The result in 40-min 3P++ (*Y*-axis) vs. 3P + (*X*-axis) analyses with 30 subjects (15 NC, open circle; 15 AD, closed circle) is shown. The k_3 estimates were empirically corrected as (3P++ k_3′) = (3P++ k_3) + (individual cerebellar k_3 by 3P+).

density theory suggested that scan time reduction to 40 min would be necessary to obtain a good fit to the 3P model [13].

When 3P + or 3P++ analysis can be applied to a ligand, such ligand is specified as a moderately reversible ligand. This applicability is determined by the information function curves of k_3 and k_4 [13], and thus is dependent on the scan time as well as k_3 and k_4 values of the ligand in a ROI. Differentiation of a moderately reversible ligand from general reversible ligands is somewhat arbitrary, though we conveniently defined this with the k_4 value (≤0.03/min) in this study.

In the present study, the 3P + plasma input model was extended to the 3P++ reference tissue input model. The 3P++ analysis has three merits over previous methods. First, the PET scan time is short, usually less than 40 min, which may be important in PET studies with elderly or demented subjects. Secondly, the target parameter k_3 can be isolated from the other model parameters. Thirdly, neither arterial cannulation nor labor-intensive measurements of labeled metabolites are required.

One of the conventional models for the estimation of binding of [^{11}C]PIB is the Logan plot analysis [2], which employs data of long duration (more than 60 min). Noninvasive Logan analysis (distribution volume ratio) [6] requires late-phase (equilibrium-phase) PET data, whereas late-phase data are not necessary for 3P++ analysis. In the noninvasive Logan model or simplified reference tissue model [8], the K_1-to-k_2 ratio in the target and reference tissues is assumed to be equal. 3P++ analysis does not require such an assumption. Since 3P++ analysis is a kind of irreversible-model analysis, K_1 (R_1) and k_3 can be independently estimated (k_2 must be fixed to a certain constant).

Noise sensitivity of 3P++ analysis

Loss of PET data in short-scan 3P++ and 3P + analyses might be considered to deteriorate the precision of the k_3 estimate. In the present simulation for noise sensitivity, k_3 CV values in 40-min 3P++ and 3P + analyses were lower than (almost three fifths of) that in 90-min 4P analysis (Figure 4), which was in accordance with the previous report [13]. It is considered that the loss of PET data may be compensated for by the reduction in the number of free parameters from four in the 4P model to three in the 3P + and 3P++ models.

K_1 effect on 3P++ analysis

In the K_1 simulation, the stableness of k_3 estimation in changes of cerebral blood flow was investigated. The magnitudes of k_3 bias were independent of the K_1 change, ranging from 0.12 to 0.24 mL/g/min, in 3P++, 3P+, and 4P analyses (Figure 5). The 3P++ as well as 3P + and 4P analyses were less affected by K_1, which is owing to the capability of isolating the k_3 estimation. The 40-min 3P + analysis showed −33% k_3 bias relative to 90-min 4P analysis, which is in accordance with the previous report [13]. In this K_1 simulation, 3P++ k_3 showed negligible bias relative to 3P + k_3. These results suggested that in 3P++ analysis, the effects of ignoring vascular volume as well as numerical integration error due to discrete time points were not significant.

Causes of negative k_3 bias in 3P++ analysis

Firstly, the k_3 bias in 3P++ analysis originates from 3P model approximation. Our previous simulation study [13] showed that the 3P + analysis with 28-min scan had large negative k_3 bias relative to 4P analysis with 90-min scan; for example, there was about −22% to −24% bias to true k_3 (4P k_3) ranging from 0.01 to 0.04/min including NC and AD k_3. 3P++ analysis showed further negative k_3 bias relative to 3P + analysis due to the following two reasons.

Secondly, the bias is due to individual k_{2r} change from the fixed value in Equation 1. In 3P++ analysis, we also assumed that k_2 in the reference tissue was constant and was fixed at 0.178/min, which was the average k_2 value with the 3P + model. In simulation, negative k_3 bias was predicted when k_{2r} was larger or smaller than fixed k_2 (Figure 6). Each subject in the NC and AD groups had different k_2 values in the reference tissue, and it is considered that such biological variance as for reference tissue may result in a negative k_3 bias in 3P++ analysis, relative to 3P + analysis for [^{11}C]PIB.

Thirdly, the bias is due to the discrepancy between the model assumption and the actual reference ROI. The basic assumption (assumption 3) in 3P++ analysis is $k_{3r} = 0$. The working equation of 3P++ analysis (Equation 1) is derived under this assumption, and reference k_3 is naturally calculated to be 0. However, in 3P + analysis with [^{11}C]PIB, the cerebellum showed nonzero k_3 (0.007 ± 0.003/min in all 30 subjects). Thus, 3P++ k_3 is expected to be underestimated. Simulation studies showed that 3P++ analysis was bias-free for ideal reference with zero k_3 and that k_3 bias became larger as k_{3r} increased (Figure 7). When k_3 was replaced by k_3', negative bias was significantly decreased in the simulation (Figure 7), as well as the slope of the regression line between 3P++ and 3P + analyses being increased from 0.461 (Figure 3A) to 0.678 (Figure 8), which also suggested that nonzero k_{3r} caused underestimation of 3P++ k_3.

Correlation of k_3 between 3P++ and 3P + analyses

Strong intra-subject k_3 correlation was shown between 3P++ and 3P + analyses, and the rank-order of k_3 was almost the same between the two analyses (Figure 2A), suggesting the stability of both 3P++ and 3P + analyses.

The inter-subject k_3 correlation (r^2; Figure 3A) was significantly lower than the intra-subject correlation (Figure 2A). Such a lower inter-subject k_3 correlation

can be partly explained by the sample variance of cerebellar k_3. In order to explain this, k_3' was calculated for each subject. When k_3 was replaced by k_3', the determination coefficient between 3P++ and 3P + analyses was increased from 0.739 (Figure 3A) to 0.975 (Figure 8); the latter is comparable to r^2 of the intra-subject k_3 correlation (0.982; Figure 2A).

Such an estimation of parameter k_3' is not always practical, as 3P + analysis with arterial input function is necessary for individual cerebellar k_3 estimation. However, these results suggest that the lower r^2 in the inter-subject correlation compared with the intra-subject correlation is due to the sample variance of cerebellar k_3 and that 3P++ analysis itself is robust, as far as the reference is ideal.

Practically, the use of mean k_{3r} may be meaningful. When target k_3 is empirically corrected as corrected k_3 = estimated k_3 + mean cerebellar k_3, the absolute bias in target k_3 would decrease. However, the precision of target k_3 would not necessarily be improved owing to the variance of individual k_{3r}.

In addition to the nonzero effect of k_{3r}, inter-subject variation of k_{2r} from the fixed value ($k_2 = 0.178$/min) may also produce individually different k_3 bias in 3P++ analysis, resulting in lower inter-subject k_3 correlation between 3P + and 3P++ analyses.

Limitations of 3P++ analysis

When 3P++ analysis was applied to [^{11}C]PIB as an example of moderately reversible ligands, a somewhat lower inter-subject k_3 correlation ($r^2 = 0.739$ or 0.711; Figure 3A or Figure 3B) was shown between the 3P++ and 3P + or 4P analyses, respectively, across a k_3 range including NC and AD (3P + k_3, 0.004 to 0.040/min). The rank order of 3P++ k_3 also differed considerably from 3P + k_3 or 4P k_3. These results were mainly due to nonzero k_{3r} and the sample variance of both k_{2r} and k_{3r} as described above. The negative k_3 bias (3P++ vs. 3P+) was larger in NC ROI (−70%) than in AD ROI (−48%) when $k_{3r} = 0.008$/min (Figure 7). The previous report showed that the difference in k_3 bias (28-min 3P + vs. 90-min 4P) was small between NC ROI (−23%) and AD ROI (−24%) [13]. Therefore, the k_3 value in 3P++ analysis may be somewhat underestimated in the ROI with lower amyloid deposition compared to 3P + or 4P analysis.

In [^{11}C]PIB PET, 3P++ analysis may be inadequate for inter-subject k_3 comparison and useful only for intra-subject (inter-ROI) comparison or pre- vs. post-comparison in the same subject. 3P++ analysis would be more suitable for such reversible ligands that have moderate k_4 and reference tissue without specific binding.

Conclusions

The 3P++ analysis is a k_3 estimation method for moderately reversible PET ligands with a short scan time such as 40 min and without arterial blood sampling. Although the applicability of 3P++ method to [^{11}C]PIB PET may be restricted to intra-subject comparison, 3P++ analysis itself is robust. The 3P++ method would be useful for PET study with non-highly reversible ligands, as far as the reference tissue without specific binding is available.

Competing interests

The authors declare that they have no competing interests.

Authors' contributions

KS participated in clinical PET study and the simulation study, and drafted the manuscript. KF conceived of the study, participated in the simulation study, and helped to draft the manuscript. HS (Shinotoh), HS (Shimada), SH, and NT participated in clinical PET study and contributed to the discussion. TS, TI, and HI supervised the design and coordination of the study. All authors read and approved the final manuscript.

Acknowledgements

The authors thank the production team staff for the production of isotopes and the PET operation staff for the acquisition of PET images.

Author details

[1]Molecular Imaging Center, National Institute of Radiological Sciences, 4-9-1 Anagawa, Inage-ku, Chiba 260-8555, Japan. [2]Department of Psychiatry, Teikyo University Chiba Medical Center, 3426-3 Anesaki, Ichihara-shi, Chiba 299-0111, Japan. [3]Neurology Chiba Clinic, 1-2-12 Benten, Chuo-ku, Chiba 260-0045, Japan. [4]Section for Human Neurophysiology, Research Center for Frontier Medical Engineering, Chiba University, 1-33 Yayoi-cho, Inage-ku, Chiba 263-8522, Japan. [5]Department of Neurology, Graduate School of Medicine, Chiba University, 1-8-1 Inohana, Chuo-ku, Chiba 260-8677, Japan. [6]Bureau of Social Welfare and Public Health, Tokyo Metropolitan Government, 2-8-1 Nishi-shinjuku, Shinjuku-ku, Tokyo 163-8001, Japan.

Received: 4 October 2013 Accepted: 6 November 2013
Published: 16 November 2013

References

1. Mintun MA, Raichle ME, Kilbourn MR, Wooten GF, Welch MJ: **A quantitative model for the in vivo assessment of drug binding sites with positron emission tomography.** *Ann Neurol* 1984, **15:**217–227.
2. Logan J, Fowler JS, Volkow ND, Wolf AP, Dewey SL, Schlyer DJ, MacGregor RR, Hitzemann R, Bendriem B, Gatley SF, Christman DR: **Graphical analysis of reversible radioligand binding from time-activity measurements applied to [N-^{11}C-methyl]-(-)-cocaine PET studies in human subjects.** *J Cereb Blood Flow Metab* 1990, **10:**740–747.
3. Hume SP, Myers R, Bloomfield PM, Opacka-Juffry J, Cremer JE, Ahier RG, Luthra SK, Brooks DJ, Lammertsma AA: **Quantification of carbon-11-labeled racropride in rat striatum using positron emission tomography.** *Synapse* 1992, **12:**47–54.
4. Innis RB, Cunningham VJ, Delforge J, Fujita M, Gjedde A, Gunn RN, Holden J, Houle S, Huang SC, Ichise M, Iida H, Ito H, Kimura Y, Koeppe RA, Knudsen GM, Knuuti J, Lammertsma AA, Laruelle M, Logan J, Maguire RP, Mintun MA, Morris ED, Parsey R, Price JC, Slifstein M, Sossi V, Suhara T, Votaw JR, Wong DF, Carson RE: **Consensus nomenclature for in vivo imaging of reversibly binding radioligands.** *J Cereb Blood Flow Metab* 2007, **27:**1533–1539.
5. Ichise M, Ballinger JR, Golan H, Vines D, Luong A, Tsai S, Kung HF: **Noninvasive quantification of dopamine D2 receptors with iodine-123-IBF SPECT.** *J Nucl Med* 1996, **37:**513–520.
6. Lammertsma AA, Hume SP: **Simplified reference tissue model for PET receptor studies.** *Neuroimage* 1996, **4:**153–158.
7. Lammertsma AA, Bench CJ, Hume SP, Osman S, Gunn K, Brooks DJ, Frackowiak RSJ: **Comparison of methods for analysis of clinical [^{11}C] raclopride studies.** *J Cereb Blood Flow Metab* 1996, **16:**42–52.
8. Logan J, Fowler JS, Volkow ND, Wang GJ, Ding YS, Alexoff DL: **Distribution volume ratios without blood sampling from graphical analysis of PET data.** *J Cereb Blood Flow Metab* 1996, **16:**834–840.
9. Watabe H, Carson RE, Iida H: **The reference tissue model: three compartments for the reference region [abstract].** *Neuroimage* 2000, **11:**S12.

10. Wu Y, Carson RE: **Noise reduction in the simplified reference tissue model for neuroreceptor functional imaging.** *J Cereb Blood Flow Metab* 2002, **22:**1440–1452.
11. Koeppe RA, Frey KA, Snyder SE, Meyer P, Kilbourn MR, Kuhl DE: **Kinetic modeling of N-[^{11}C]methylpiperidin-4-yl propionate: alternatives for analysis of an irreversible positron emission tomography tracer for measurement of acetylcholinesterase activity in human brain.** *J Cereb Blood Flow Metab* 1999, **19:**1150–1163.
12. Namba H, Iyo M, Fukushi K, Shinotoh H, Nagatsuka S, Suhara T, Sudo Y, Suzuki K, Irie T: **Human cerebral acetylcholinesterase activity measured with positron emission tomography: procedure, normal values and effect of age.** *Eur J Nucl Med* 1999, **26:**135–143.
13. Sato K, Fukushi K, Shinotoh H, Shimada H, Tanaka N, Hirano S, Irie T: **A short-scan method for k_3 estimation with moderately reversible PET ligands: application of irreversible model to early-phase PET data.** *Neuroimage* 2012, **59:**3149–3158.
14. Price JC, Klunk WE, Lopresti BJ, Lu X, Hoge JA, Ziolko SK, Holt DP, Meltzer CC, DeKosky ST, Mathis CA: **Kinetic modeling of amyloid binding in humans using PET imaging and Pittsburgh Compound-B.** *J Cereb Blood Flow Metab* 2005, **25:**1528–1547.
15. Gunn RN, Gunn SR, Cunningham VJ: **Positron emission tomography compartmental models.** *J Cereb Blood Flow Metab* 2001, **21:**635–652.
16. McKhann G, Drachman D, Folstein M, Katzman R, Price D, Stadlan EM: **Clinical diagnosis of Alzheimer's disease: report of the NINCDS-ADRDA work group under the auspices of Department of Health and Human Services Task Force on Alzheimer's Disease.** *Neurology* 1984, **34:**939–944.
17. Mathis CA, Wang Y, Holt DP, Huang G-F, Debnath ML: **Synthesis and evaluation of ^{11}C-labeled 6-substituted 2-aryl benzothiazoles as amyloid imaging agents.** *J Med Chem* 2003, **46:**2740–2754.
18. Logan J, Fowler JS, Volkow ND, Ding YS, Wang GJ, Alexoff D: **A strategy for removing the bias in the graphical analysis method.** *J Cereb Blood Flow Metab* 2001, **21:**307–320.
19. Blomquist G, Englar H, Nordberg A, Ringheim A, Wall A, Forsberg A, Estrada M, Franberg P, Antoni G, Langstrom B: **Unidirectional influx and net accumulation of PIB.** *Open Neuroimag J* 2008, **2:**114–125.

doi:10.1186/2191-219X-3-76
Cite this article as: Sato *et al.*: Noninvasive k_3 estimation method for slow dissociation PET ligands: application to [^{11}C]Pittsburgh compound B. *EJNMMI Research* 2013 **3**:76.